CONTRACT TECHNICAL REPORT

"TRANSVERSE CRACKING AND DELAMINATION IN CROSS-PLY GR/EP COMPOSITES UNDER DRY, SATURATED AND IMMERSED FATIGUE"

By

Alex S. Selvarathinam and Y. Jack Weitsman

Prepared for: Office of Naval Research
Arlington, Virginia

Mechanics Division
Engineering Science Directorate
Contract N00014-96-1-0821

Report MAES97-4.0-CM
November 1997

Mechanical and Aerospace Engineering and Engineering Science
THE UNIVERSITY OF TENNESSEE
Knoxville, TN 37996-2030

Unclassified

SECURITY CLASSIFICATION OF THIS PAGE

REPORT DOCUMENTATION PAGE

1a. REPORT SECURITY CLASSIFICATION Unclassified	1b. RESTRICTIVE MARKINGS
2a. SECURITY CLASSIFICATION AUTHORITY	3. DISTRIBUTION/AVAILABILITY OF REPORT Unlimited
2b. DECLASSIFICATION/DOWNGRADING SCHEDULE	
4. PERFORMING ORGANIZATION REPORT NUMBER(S)	5. MONITORING ORGANIZATION REPORT NUMBER(S)
6a. NAME OF PERFORMING ORGANIZATION Mechanical & Aerospace Engr. & Engr. Sci. University of Tennessee 6b. OFFICE SYMBOL (If applicable)	7a. NAME OF MONITORING ORGANIZATION Office of Naval Research
6c. ADDRESS (City, State and ZIP Code) 307 Perkins Hall Knoxville, TN 37996-2030	7b. ADDRESS (City, State and ZIP Code) Office of Naval Research, code 432 800 N. Quincy Ave., BCT #1, Room 528 Arlington, VA 22217
8a. NAME OF FUNDING/SPONSORING ORGANIZATION Office of Naval Research 8b. OFFICE SYMBOL (If applicable)	9. PROCUREMENT INSTRUMENT IDENTIFICATION NUMBER N00014-96-1-0821 (ONR Contract #)
8c. ADDRESS (City, State and ZIP Code) Arlington, VA 22217	10. SOURCE OF FUNDING NOS. PROGRAM ELEMENT NO. / PROJECT NO. / TASK NO. / WORK UNIT NO.
11. TITLE (Include Security Classification) "Transverse Cracking and Delamination in Cross-Ply Gr/Ep Composites Under Dry, Saturated and Immersed Fatigue"	
12. PERSONAL AUTHOR(S) Alex S. Selvarathinam and Y. Jack Weitsman	
13a. TYPE OF REPORT Technical 13b. TIME COVERED FROM 2/1/97 TO 9/30/98	14. DATE OF REPORT (Yr., Mo., Day) 97-11-18 15. PAGE COUNT 16
16. SUPPLEMENTARY NOTATION	
17. COSATI CODES FIELD / GROUP / SUB. GR.	18. SUBJECT TERMS (Continue on reverse if necessary and identify by block number)

19. ABSTRACT (Continue on reverse if necessary and identify by block number)

Motivated by experimental observations, the finite element method is employed to model the competition between the transverse cracking and delamination modes of failure that occur in cross-ply AS4/3501-6 gr/ep coupons subjected to fatigue. The results explain the extensive delaminations and reduced crack densities that arise under immersed fatigue, as compared with fatigue in air.

20. DISTRIBUTION/AVAILABILITY OF ABSTRACT UNCLASSIFIED/UNLIMITED ☐ SAME AS RPT. ☐ DTIC USERS ☐	21. ABSTRACT SECURITY CLASSIFICATION Unclassified
22a. NAME OF RESPONSIBLE INDIVIDUAL Dr. Yapa Rajapakse	22b. TELEPHONE NUMBER (Include Area Code) (703) 696-4405 22c. OFFICE SYMBOL

DD FORM 1473, 83 APR EDITION OF 1 JAN 73 IS OBSOLETE.

Unclassified

SECURITY CLASSIFICATION OF THIS PAGE

TRANSVERSE CRACKING AND DELAMINATION IN CROSS-PLY GR/EP COMPOSITES UNDER DRY, SATURATED AND IMMERSED FATIGUE

Alex S. Selvarathinam and Y. Jack Weitsman
Department of Mechanical & Aerospace Engineering & Engineering Science
307 Perkins Hall, University of Tennesee
Knoxville, Tennessee 37996-2030

Abstract

Motivated by experimental observations, the finite element method is employed to model the competition between the transverse cracking and delamination modes of failure that occur in cross-ply AS4/3501-6 gr/ep coupons subjected to fatigue. The results explain the extensive delaminations and reduced crack densities that arise under immersed fatigue, as compared with fatigue in air.

1 Introduction

The effects of fluids on polymers and polymeric composites have been studied extensively over the past several decades. Recently, the subject received a new impetus due to the revived interest in utilizing composites in marine, automotive, and civil structures. A recent review of the literature (Weitsman, 1995) indicates that relatively little information is available regarding the fatigue response of composites in "wet" conditions, and that the sparse amount of reported data concerns pre-saturated samples fatigued in air.

Recent experiments (Kosuri and Weitsman, 1995; Gao and Weitsman, forthcoming) on the fatigue response of $[0°/90°_3]_s$ AS4/3501-6 gr/ep coupons suggest that the fatigue life of pre-saturated samples subjected to cyclic loading under immersed conditions is reduced by up to one decade in comparison with that of dry coupons fatigued in air. Pre-saturated coupons fatigued in air appear to possess the longest fatigue life. Perhaps more remarkably, detailed observations of failed coupons have shown that, when compared with the dry case, the saturated-immersed circumstance resulted in substantially larger delaminations at the 0°/90° interfaces and with notably fewer transverse cracks (i.e. lesser crack density) in the 90° ply group. Typical observations are shown in Fig. 1. (Gao and Weitsman, forthcoming).

The above mentioned experiments utilized simulated sea water. They were performed at a frequency of 5 Hz, with R ratios ($R = \sigma_{min}/\sigma_{max}$) of 0.01, 0.1 and 0.3 and at σ_{max} levels of 400, 425, 450 and 475 MPa (The average value of the

coupons' ultimate failure stress was 540 MPa). The computations below correspond to σ_{max} = 450 MPa and R= 0.1, i.e. σ_{min} = 45 MPa.

Additional experiments were performed to assess the rate of capillary climb in the transverse cracks within the 90° ply group (work by Kosuri, reported by Smith and Weitsman, 1996). Observations suggest that such motion proceeds at approximately 5×10^{-5} m/sec, thus requiring about 250 sec. to extend over the entire lengths of the transverse cracks in one inch (25×10^{-3} m) wide coupons immersed in sea water. This time span exceeds the time-interval for one periodic oscillation in the fatigue load by three orders of magnitude. Thus $t^* = t_{capillary}/t_{fatigue} \approx 10^3$.

2 Basic Considerations

It is assumed that in the immersed fatigue case water enters all transverse cracks by capillary motion and random walk process. Subsequently, the water contained within the cracks cannot escape into the ambient during the down-loading stages of the fatigue cycle in view of the aforementioned value of $t^* \approx 10^3$. Thus, the water trapped within the transverse cracks is squeezed into all weak regions within the composite sample during the down-loading stages, these regions being the 0°/90° interfaces. Consequently, the maximal levels of delamination fracture energy in immersed samples occur when the pressure p on the crack surfaces is at its peak value, namely when $\sigma = \sigma_{min}$. On the other hand, at $\sigma = \sigma_{max}$ the cracks are fully open and p = o.
The above reasoning does not apply to fatigue in air, in which case delaminations are attributable to stresses near or at $\sigma = \sigma_{max}$. The density of transverse cracks is associated with σ_{max} for both dry and immersed cases, when the available fracture energy for that failure mode is largest.

Turning to fracture processes it is hypothesized that all transverse cracks, which span the inner 90° ply-group, are equally spaced and that they terminate just short of the 0°/90° interface. It is also assumed that all delaminations emanate from the tips of all transverse cracks and grow in unison along the 0°/90° interfaces, as shown in fig. 1.

The idealized assumptions of equal spacing and simultaneous growth of delaminations are made to retain computational tractability, since they allow us to restrict attention to a periodic, "unit cell" geometry. The assumption that transverse cracks do not impinge on the 0°/90° interface is borne out by experimental evidence. This assumption, which greatly simplifies the considerations of crack-tip singularity, can be further justified by the realization that no sharp boundary exists at the 0°/90° interfaces of cross-ply composites.

In addition, it is considered that transverse cracks are constituted at first across the thickness of the 90° ply-group and subsequently grow in a straight

front along the width of the specimen as tunneling cracks. This assumption is also borne out by experimental evidence.

Finally, the analysis is restricted to the evaluation of available levels of fracture energies in several static states and does not consider fatigue effects on crack growth.

3 Analysis

3.1 Geometry and Material Properties

In view of the aforementioned considerations, attention is confined to the representative cell indicated in Fig. 2. In that figure h = 0.5 mm (half the coupon's thickness) and L = 12 mm. The length L, which is the initial value of half the spacing between transverse cracks, was chosen after some preliminary computational work which indicated that crack interactions are insignificant at spacings that exceed L = 12 mm. The coupon's width w=25mm plays no role in the sequel, since we consider the state of plane strain. Both y and z axes in Fig. 2 serve as symmetry lines for analysis that follows.

The Following material properties and hygro-thermal coefficients are assumed: E_1 = 139GPa, $E_2 = E_3$ =11Gpa, $\nu_{12} = \nu_{13} = 0.27$, $\nu_{23} = 0.34$, G_{12} = 4.8GPa, $G_{23} = \frac{E_3}{2(1+\nu_{23})}$, α_1 =- 0.9με/°C, α_2 = 31με/°C, β_1 = 100με/%Δw, β_2 = 3200με/%Δw. In the above 1 indicates fiber direction and fiber direction and 2 and 3 are mutually perpendicular to it. E_i, ν_{ij}, i, j = 1,2,3 are the stiffnesses and Poissons' ratios respectively, and G_{12} and G_{23} are the shear moduli in the 1-2 and 2-3 planes. α_i's and β_i's are the thermal and hygral coefficients of expansion, respectively.

Only meager information is available regarding the effects of water on the levels of critical fracture energy in polymeric composites (Chou, I., et. al., 1993) Consequently, we assume that the same values apply to both dry and wet cases.

3.2 Finite Element Scheme

All computations were initiated at the reference configuration shown in Fig. 1. Eight node quadrilateral, plane strain elements were used over most of the domain except near the crack tips, where six node triangular plane strain elements were incorporated. PATRAN [version 5, MSC 1996] was used to generate the mesh and develop the model and ABAQUS [version 5.4, Hibbit, Karlsson and Sorensen Inc. 1994] was employed to solve the resulting finite element system.

As noted earlier the initial spacing of transverse cracks, L = 12 mm, was considered to undergo a sequence of equal subdivisions under fatigue loading. At each stage of that sequel the presence of delaminations, as well as their growth, was also considered. A typical circumstance is shown in Fig. 3, depicting a transverse crack spacing of 2L = 3 mm and delaminations of equal lengths a. In accordance with the basic considerations listed earlier the transverse cracks were stopped at a distance $\delta = 7.8125\,\mu$ short of the interface, which corresponds to the fiber diameter. Furthermore, when calculating energy release rates along the 0°/90° interfaces the limiting process as $\Delta a \rightarrow 0$ was terminated at $\Delta a = 0.1\delta$, judging this to be the smallest reasonable physical dimension in the present case. Consequently, the smallest elements employed in this work were of lengths δ, and 0.1δ as noted above.

Finally, it is worth mentioning that in all circumstances it was ascertained that no interpenetration occured across opposing crack faces.

3.3 Stress States and Boundary Conditions

The case of dry fatigue was simulated by accounting for mechanical stresses and residual thermal stresses. The mechanical stresses were evaluated under peak loads, i.e. $\bar{\sigma}_y = \sigma_{max} = 450$ MPa, and the residual thermal stresses corresponded to a temperature excursion $\Delta T = -125°C$, accounting for post-processing cool down. In that case the surfaces of the transverse cracks were considered to be traction free.

Similar considerations applied to the case of saturated specimens fatigued in air, except that the residual stresses included the effects of a uniform moisture profile of w = 1.7%. Note that all surfaces of transverse cracks are still taken to be traction free and the largest impetus for growth of both damage mechanisms, transverse cracking and delaminations, occurs at $\bar{\sigma} = \sigma_{max}$.

The case of immersed fatigue differs from the above circumstances in view of the fact that the water entrapped within the cracks induces a hydrostatic pressure on all crack faces at all levels of applied stress $\bar{\sigma} < \sigma_{max}$. This pressure vanishes at $\bar{\sigma} = \sigma_{max}$, when the fully open cracks can freely accommodate the enclosed water, and attains its largest value at $\bar{\sigma} = \sigma_{min}$. Consequently, while the highest impetus for further transverse cracking still occurs at $\bar{\sigma} = \sigma_{max}$, delamination growth is driven by both the external mechanical stress $\bar{\sigma}$ and the now present internal pressure p. Although it is conceivable that maximal growth could occur at some intermediate level of σ, namely $\sigma_{min} < \sigma < \sigma_{max}$, corresponding to $p_{max} > p > o$, preliminary computations with a simpler model (Smith and Weitsman, 1996) suggest that it is reasonable to consider $\bar{\sigma} = \sigma_{min}$ whereby $p = p_{max}$, as the extreme circumstance for the instigation of delamination growth.

The pressure p is evaluated by the iterative procedure outlined below:

As a first step the volume V_i of the fully open cracks, when $\bar{\sigma} = \sigma_{max}$ and $p = o$, is evaluated through the finite element analysis. Subsequently, three levels of hydrostatic pressure p are applied to the crack surfaces together with $\bar{\sigma} = \sigma_{min}$, with corresponding crack volumes V_f computed for all three cases.

The results are correlated by a quadratic expression

$$V_f = ap^2 + bp + c \tag{1}$$

thus a, b, and c are know constants.

The volumetric change between σ_{max} and σ_{min} is related to p through the bulk modulus K_w of water (K_w = 2.5GPa), thus

$$p = K_w \frac{V_f - V_i}{V_i} \tag{2}$$

Expressions (1) and (2) yield the value of p via

$$p^2 + p\,\frac{K_w b - V_i}{K_w a} + \frac{c - V_i}{a} = o \tag{3}$$

Obviously, it is possible to determine p by direct iteration. Comparative calculations resulted in good agreements with the scheme outlined above, which proved to be much more efficient.

4 Fracture Energy Analysis

4.1 Transverse Cracks

As noted earlier, these cracks are assumed to grow in a "tunneling" fashion in the width direction of the coupon. Considering the steady state growth of new cracks mid-way between pre-existing cracks that are spaced at distance 2λ apart, straightforward considerations (e.g. Weitsman and Zhu, 1993; Erdman and Weitsman, forthcoming) yield the following expression for the available fracture energy release rate

$$G_I = \frac{2U(\lambda) - U(2\lambda)}{2c} \tag{4}$$

where $U(\lambda)$ and $U(2\lambda)$ denote the strain energies in representative cell that correspond to crack spacings of λ and 2λ, respectively and 2c is the length of the crack front, (c = 0.75h in the present analysis). Note that only mode I fracture energy obtains for transverse cracking.

It should be noted that the crack opening displacements, and hence also the volume enclosed between opposing crack faces, may diminish upon the formation of new transverse cracks. This implies that, for expression (4) to hold, some of the water entrapped within previously established cracks is assumed to be squeezed out during ongoing fatigue. This apparently reasonable assumption is necessary to maintain computational tractability.

4.2 Delaminations

Delaminations are assumed to grow in unison parallel to the 0°/90° interfaces as shown in Fig. 2. They are considered to be completely established along the specimen's width.

Mode I and Mode II energy release rates, $G_I^{delam.}$ and $G_{II}^{delam.}$, are evaluated employing the virtual crack extension method (Ribicki and Kanninen, 1977) and its subsequent refinements (Raju, 1987; Raju, Crews and Aminpour, 1988). The above quantities are computed for every configuration of transverse cracks and for delaminations of increasing lengths a in the range $\delta < a < \lambda - \delta$, where δ denoted the fiber diameter as before. Note that the presence of the delimiting dimensional scale δ enables us to disregard the oscillatory singularity at the tip of the delamination and thereby determine both G_I and G_{II}.

As mentioned earlier, delaminations in the case of immersed fatigue were evaluated at $\bar{\sigma} = \sigma_{min}$, which corresponds to a hydrostatic pressure $p = p_{max}$ over the crack surfaces. This circumstance required the computation of V_i, and the subsequent evaluation of $p = p_{max}$ according to Eqs. (1)-(3), for each configuration of transverse cracks and at all delamination lengths.

4.3 Fracture Criteria

In the case of transverse cracking, new cracks are assumed to occur when

$$G_I = G_{IC} \qquad (5)$$

with G_I given in Eqn. (4).

Delamination growth is considered to occur when

$$G_{total}^{delam.} = G_I^{delam.} + G_{II}^{delam.} = G_C \quad (6)$$

where

$$G_C = G_C(G_I^{delam.}, G_{II}^{delam.}) \quad (7)$$

as suggested recently. (O'Brien, 1997).

Obviously, the actual values of $G_I^{delam.}$ and $G_{II}^{delam.}$ depend on the spacing of transverse cracks, as well as on the delamination length a.

The competition between further transverse cracking and increasing delaminations at a stabilized configuration of transverse cracks is determined by comparing criteria (5) and (6). For prescribed values of σ_{max} and σ_{min} the competition settles at some fixed configuration of transverse cracks, beyond which $G_{total}^{delam.}/G_c > G_I/G_{IC}$ and delamination becomes the preferred mode of failure.

5 Results

Results for the dry case, and for the fully saturated coupons fatigued in air and under immersed conditions, are exhibited by the pairs of surfaces shown in Figs. 4, 5, and 6, respectively. These surfaces correspond to $g = G_{available}/G_{critical}$ for transverse cracking and for delaminations, plotted vs. the density of transverse cracks and of delamination length. With the exception of g for delamination in the case of immersed fatigue (the upper surface in Fig. 6), which corresponds to $\bar{\sigma} = \sigma_{min} = 45$ MPa, all other surfaces comport with $\bar{\sigma} = \sigma_{max} = 450$ MPa. Note that, as a consequence of our assumption that transverse cracking precedes delamination, the progression of transverse cracking is independent of delamination length and is described by the developable surfaces in Figs. 4, 5, 6.

For added clarity the intersections of the three pairs of surfaces in the foregoing figures are re-drawn in Fig. 7, exhibiting the switching from transverse cracking to delamination. Note that the various curves in Fig. 7 emanate from disparate levels of transverse crack densities at points A, B and C, namely 0.52 mm^{-1}, 0.89 mm^{-1} and 0.9 mm^{-1}, respectively. In all circumstances the initiation of delamination is followed by delamination growth, since $G/G_c > 1$ at A, B, and C. However, while delamination arrest is predicted for fatigue in air (curves DIA and SI), when $G/G_c = 1$, unrestricted growth is predicted for the saturated immersed case (curve SI). The calculated density of transverse cracks for the DIA case (0.89 mm^{-1}) compares well with experimental observations (1.0 mm^{-1}). However, experimental observations indicate that a higher crack density (0.3 mm^{-1}) occurs in the SI case than predicted in the present article (i.e. 0.52 mm^{-1}). The disparity suggests that G_c in the immersed case is lower than that in the dry case, in contrast to the presumed equality

employed in the calculations. However, no G_c data are available for the immersed case.

6 Concluding Remarks

A detailed finite element analysis was performed to evaluate the competition between the progression of transverse cracking and interfacial delaminations in cross-ply gr/ep coupons subjected to fatigue. The analysis considered the circumstances of fatigue in air, for both dry and water-saturated samples, and of the immersed fatigue of saturated coupons. An accounting for fatigue was attained by evaluating available fracture energies at the maximal and minimal load levels during cycling.

To maintain tractability the analysis employed idealized geometric configurations that assume symmetric formations of both transverse cracks and delaminations. While such idealizations tend to overestimate all levels of available fracture energy, when compared with realistic circumstance which involve fewer cracks, this trend may be compensated by the fact that the bending which arises in the absence of symmetry may greatly enhance the foregoing energy levels.

It is interesting to note that the model and results presented herein, which involved static analyses, agree, at least qualitatively, with experimental observations.

Acknowledgement

This work was conducted under Contract No: Navy N00014-96-1-0821, from the Office of Naval Research. The support of Dr. Y. Rajapakse, the Program Manager, is gratefully acknowledged.

References

[1] Gao, J. and Weitsman, Y.J., "The Dry and Immersed Fatigue of Cross-Ply Gr/Ep. Composites", (Forthcoming)

[2] Chou, I., Kimpara, I., Kageyama, K. and Ohsawa, I. (1993): "Effect of Moisture Absorption on Mode I and Mode II Interlaminar Fracture Toughness of CFRP Laminates", pp. 8-16, Japan Journal of Composite Materials *(In Japanese)*.

[3] Kosuri, R. and Weitsman, Y., (1995). "Sorption Processes and Immersed Fatigue Response of Gr/Ep Composites in Sea Water," Proceedings of the ICCM-10, Whistler, British Columbia, Canada, August 14-18, 1995. Vol. VI. pp. 177-184.

[4] O'Brien, T.K. (1997). "Composite Interlaminar Shear Fracture G_{IIC}: Shear Measurement or Shear Myth?" NASA Technical Memorandum 110280. U.S. Army Laboratory Technical Report 1312.

[5] Raju, I.S. (1987). "Calculation of Strain-Energy Release Rates with Higher Order and Singular Finite Elements". *Engineering Fracture Mechanics*, Vol. 28, pp. 251-274.

[6] Raju, I.S., Crews Jr., H.H., and Aminpour, M.A., (1988). "Convergence of Strain Energy Release Rate Components for Edge-Delaminated Composite Laminates". *Engineering Fracture Mechanics*, Vol. 30, pp. 383-396.

[7] Rybicki, E.F. and Kanninen, M.F., (1977). "A Finite Element Calculation of Stress Intensity Factors by a Modified Crack Closure Integral". *Engineering Fracture Mechanics* 9:931-938.

[8] Smith, L.V. and Weitsman, Y. J. (1996). "The Immersed Fatigue Response of Polymer Composites", International Journal of Fracture, Vol. 82, pp. 31-42.

[9] Weitsman, Y., (July 1995). "Effects of Fluids on Polymeric Composites - A Review", Report No. NAES 95-1.0-CM, Department of Mechanical and Aerospace Engineering and Engineering Science, University of Tennessee, Knoxville, TN 37996-2030.

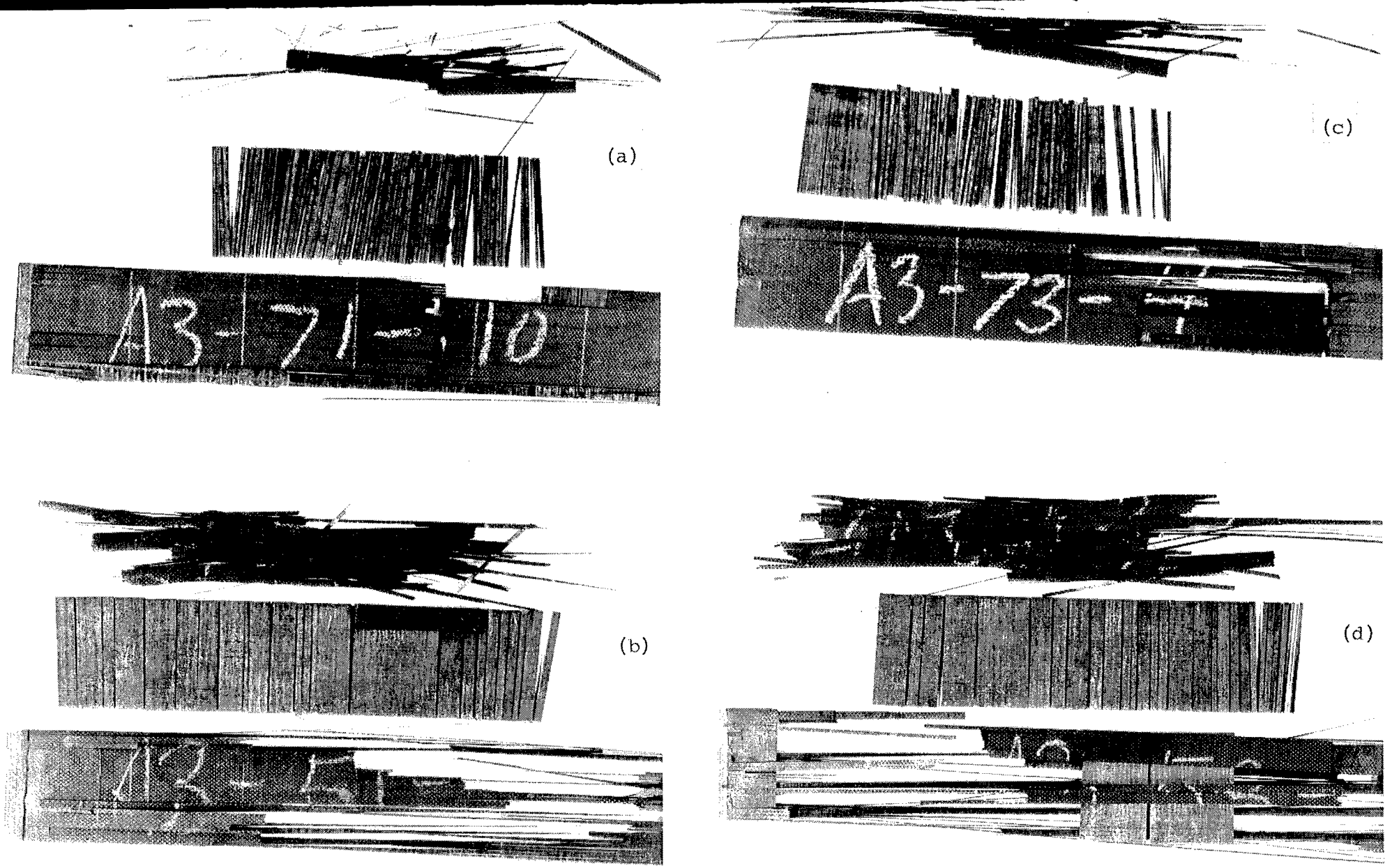

Fig. 1. Observations of Transverse cracks in the 90° Ply-Group Delaminations at the 0°/90° Interfaces of Failed $[0°/90°_3]_s$ gr/ep Coupons Subjected to Fatigue. The Peeled-Off Portion of the 0° Ply is shown on the Top of Each Photo, Indicating Extent of Delamination. (a) Dry and (b) Saturated Immersed for $\sigma_{max} = 0.8\sigma_u$. (c) Dry and (d) Saturated Immersed for $\sigma_{max} = 0.85\sigma_u$. In all cases $R = \sigma_{min}/\sigma_{max} = 0.1$.

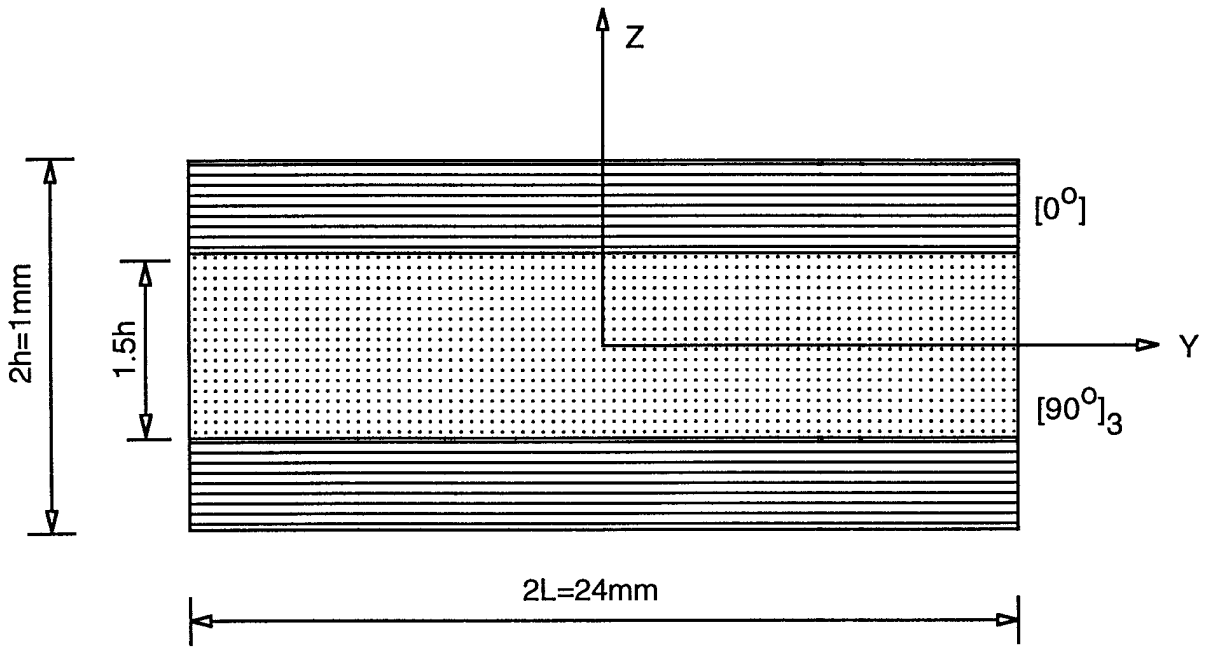

Fig.2 The Representative Geometry Employed in the Finite Element Analysis with the Representative Cell Occupying the Quadrant $0 \leq Y \leq L$, $0 \leq Z \leq h$

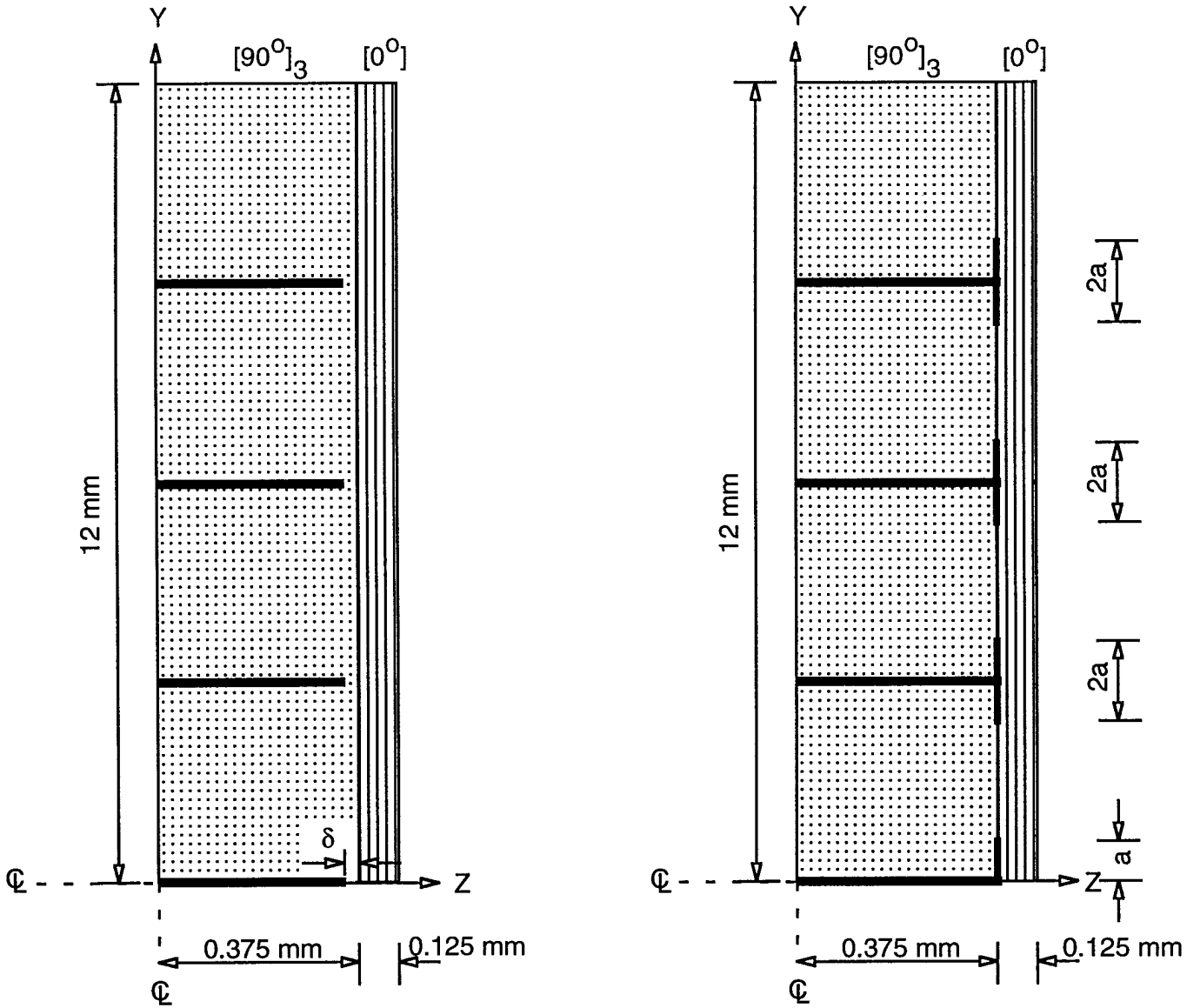

Fig. 3 The Geometry of the Finite Element Model Used for Modelling (a) Transverse Cracks and (b) Delaminations (δ=7.8125μ)

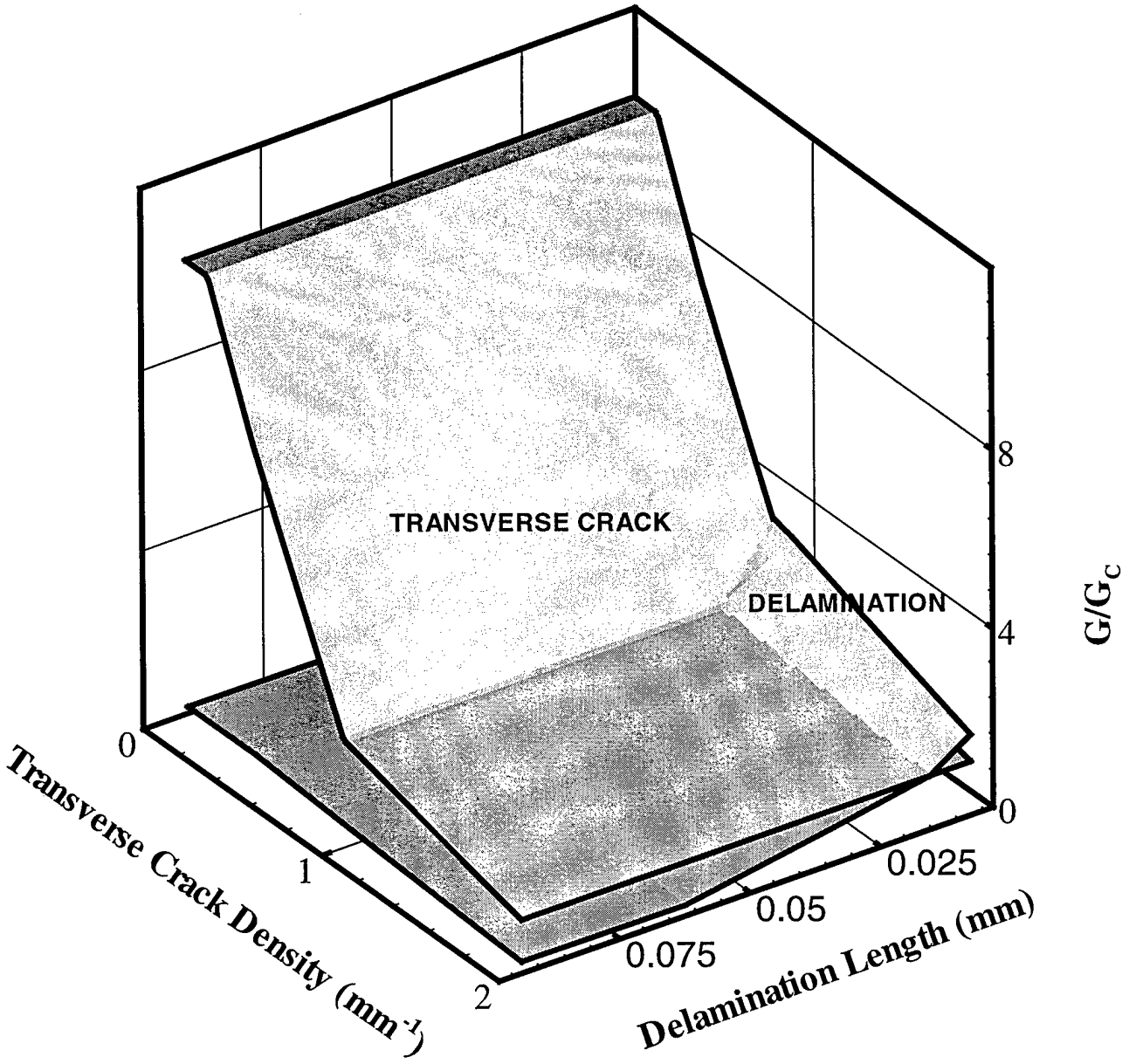

Fig.4. Available Fracture Energies, scaled by the required levels, for Transverse Cracking and for Delamination at the maximal stress level (σ=450 MPa) of Dry Fatigue, vs. Density of Transverse Cracks and Delamination Lengths in a $[0°/90°_3]_s$ gr/ep coupon.

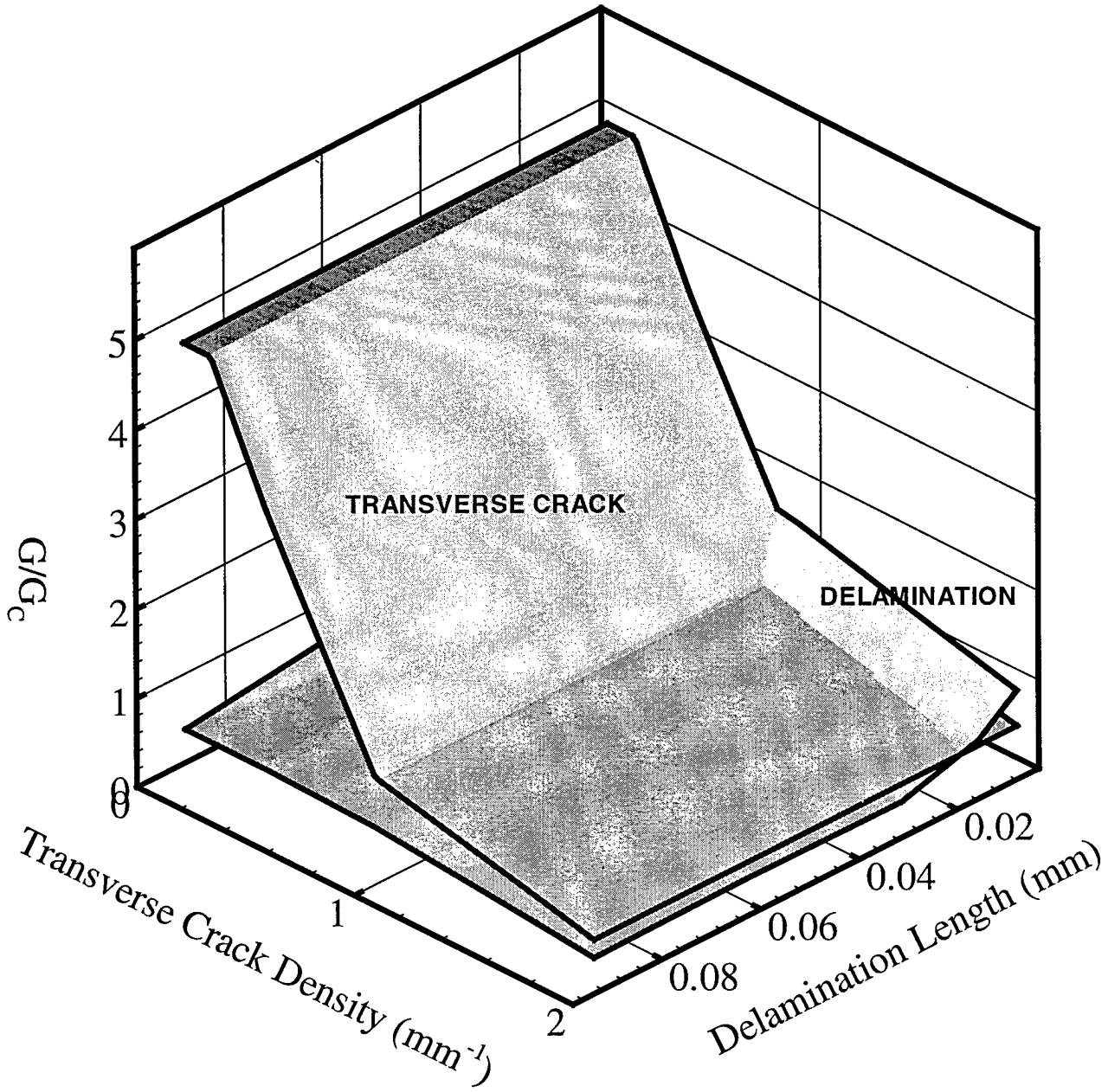

Fig 5. Available Fracture Energies, scaled by the required levels, for Transverse Cracking and for Delamination at the maximal stress level (σ=450 MPa) of saturated coupons fatigued in air, vs. Density of Transverse Cracks and Delamination Lengths in a $[0°/90_3^c]_s$ gr/ep coupon.

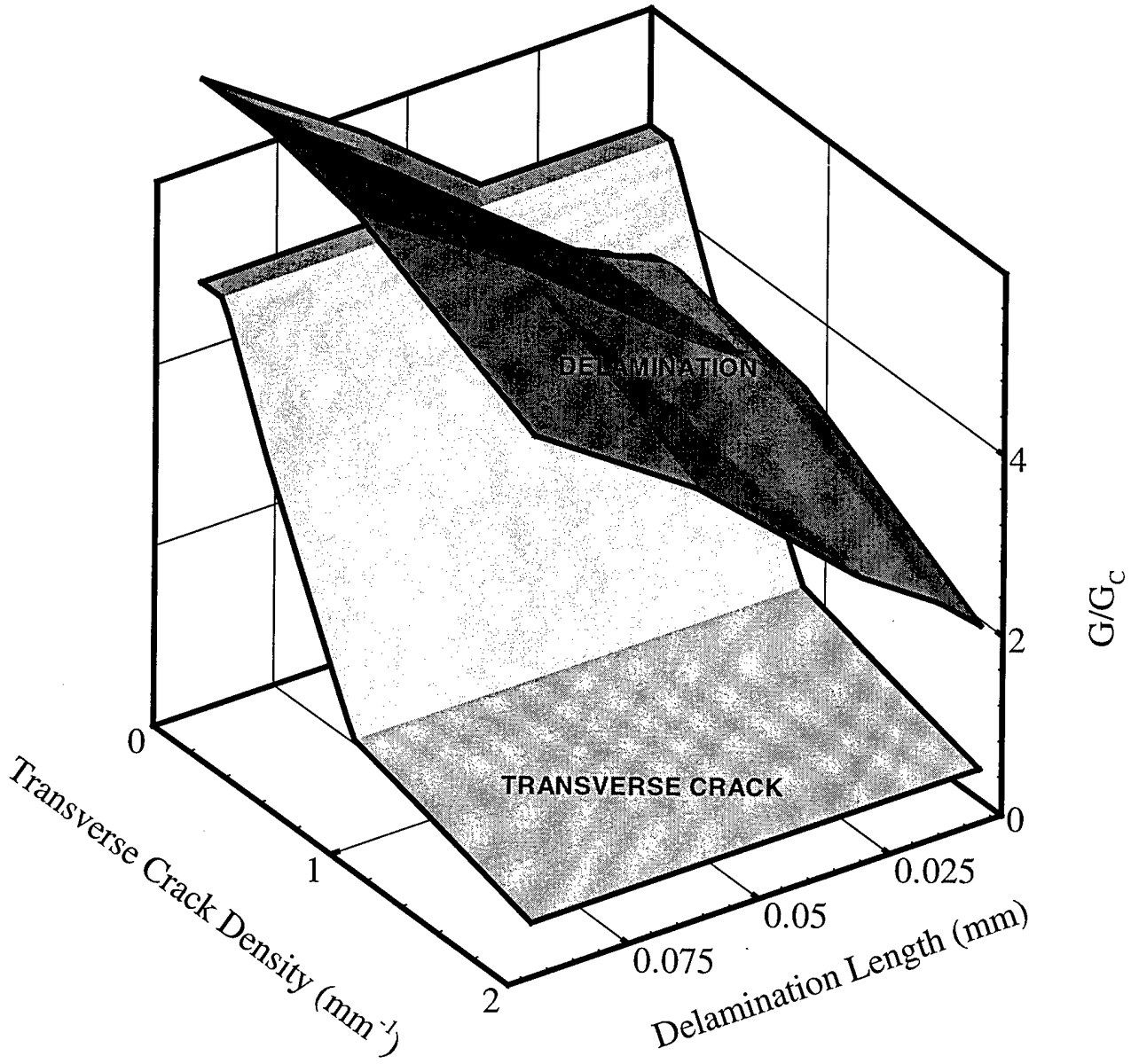

Fig. 6. Available Fracture Energies, scaled by required levels, for Transverse Cracking at the maximal stress level (σ=450 MPa) and for Delamination at the Downloading stage (σ=45 MPa) of Immersed Fatigue vs. Density of Transverse Cracks and Delamination Lengths in $[0°/90°_3]_s$ gr/ep coupons.

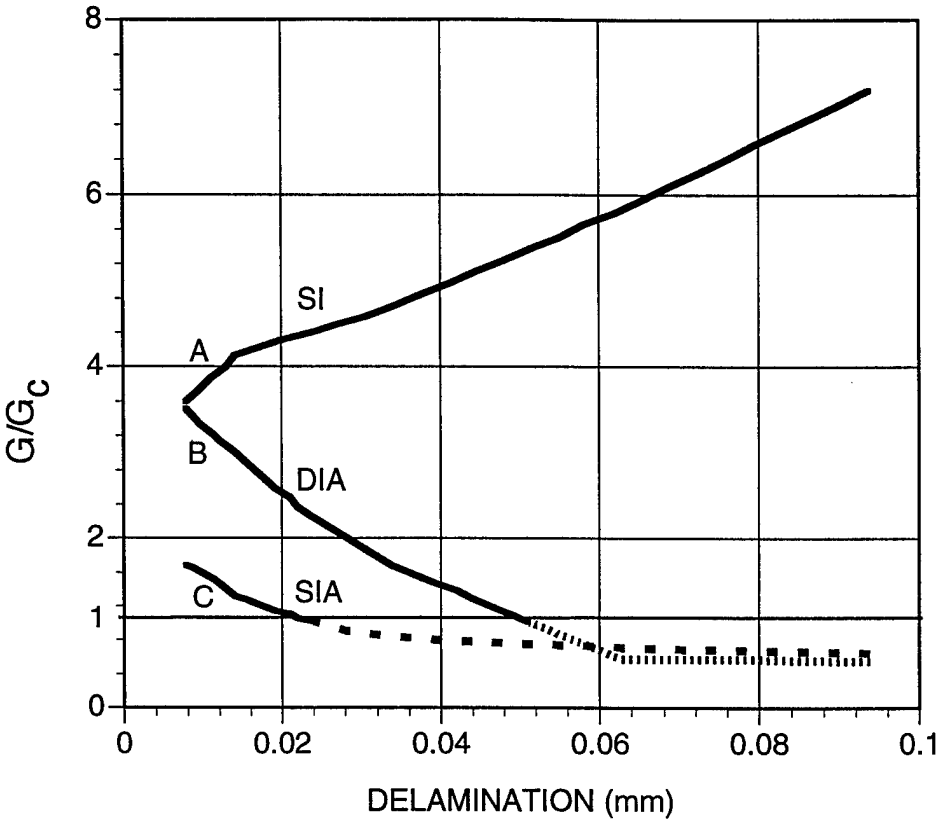

Fig. 7. The Intersection Curves of the surfaces shown in Figs. 5, 6, and 7, indicated by DIA ("Dry in Air"), SIA ("Saturated in Air"), and SI ("Saturated immersed"), respectively. These Curves exhibit the trends towards increasing delaminations upon switching from failure by transverse cracking. Note that the above curves emanate from distinct values A,B,C of transverse crack density. Also, Delamination Arrest is predicted for the DIA and SIA cases, when $G/G_c \leq 1$, while no arrest is predicated for the SI case.